Vol. 41, No. 4 (2019) 537-547, DOI: 10.24874/ti.2019.41.04.07

Tribology in Industry

www.tribology.rs

RESEARCH

Experimental Studies on Mechanical and Wear Behaviour of TiC Reinforced Cu-Sn-Ni Functionally Graded Composite

N. Radhika[a,*], M. Sam[a], S. Thirumalini[a]

[a] *Department of Mechanical Engineering, Amrita School of Engineering-Coimbatore, Amrita Vishwa Vidyapeetham, India – 641112.*

Keywords:

Copper Functionally Grade Composite
Grain Nucleation
Tribolayer
Non-lubricated Tribology
Fractography
Tribo-Mechanism

* Corresponding author:

N. Radhika
E-mail: n_radhika1@cb.amrita.edu

Received: 2 November 2018
Revised: 18 February 2019
Accepted: 29 May 2019

A B S T R A C T

This research aims to fabricate Cu-10Sn-5Ni /10wt%TiC functionally graded composite (Øout100 X Øin70 X 100 mm) through horizontal centrifuge cast technique and to study its tribo-mechanical characteristics. Microstructural observation revealed higher percentile of reinforcement particles at inner wall zone compared to middle and outer zones. Vicker's micro hardness tests revealed proportional increase of hardness along the radial wall towards inner periphery. Inner (7-15 mm) zone had higher tensile strength (291 MPa) compared to outer (1-7 mm) zone (236 MPa). Non-lubricated tribology experiments were performed at inner, middle and outer region of composite using pin-on-disc tribometer under a wide range of loads, sliding distances and sliding velocities. From the wear experiment results, it was observed that inner region had minimal wear due to rich particle presence. Scanning Electron Microscopy on worn specimen at low and high wear parametric conditions exhibited features like delamination, ploughing, micro cutting, particle pull-out, plastic deformation with flaky wear debris and thin film formation.

1. INTRODUCTION

Large technological improvement requires a holistic development in materials, which is required to meet the desired properties for promising applications. Metal Matrix Composites (MMCs) are found to be of growing demand in industrial sector due to its superior mechanical and thermal characteristics [1,2]. Copper MMCs in tribological application have attracted considerable interest by many industries and nuclear fields for the past two decades [3-5]. It also exhibit superior combination of high hardness, heat resistance and tensile strength [6]. Those copper MMCs are produced by numerous techniques such as powder metallurgy, liquid metal infiltration, in-situ process, squeeze casting, diffusion bonding, spray forming and electro- deposition method [7]. An evaluation on adhesive tribo-mechanical characteristics of pure copper reinforced with varied wt.% (0, 5, 10 and 20) of potassium acid

titanate whisker; fabricated by hot pressing revealed maximum tensile strength with 5 wt % reinforcement, whereas wear resistance was higher at 10 wt.% whisker content [8]. On analysing the effect of increasing volume fraction (9.3 to 23.3 %) of short carbon fibers on the tribo-mechanical characteristics of copper MMCs synthesized through cold press followed by sintering technique, it was concluded that the sliding tribology and mechanical properties of the composite increased with increasing volume fraction of short carbon fibers [9]. Anlaysing the effect of SiC (silicon carbide) (10 and 20 vol.%) on the wear behaviour of pure Cu/SiC MMCs concluded that 20 vol.% SiC/Cu composite had the highest wear resistance when synthesised through powder metallurgy [10]. Tribological behaviour of pure copper when hot-pressed with varied vol.% of Ti_2SnC particles (5 to 30) exhibited maximum wear resistance at Cu/10 vol.% Ti_2SnC particles under 30N applied load and 2 m/min slide velocity [11].

Functionally Graded Material (FGM) is an advanced novel material developed, which offers superior combination of material characteristics that often lack with conventional monolithic alloys. FGMs are characterized by the formation of gradient structure across its dimensions [12,13]. It is produced by many processing techniques such as centrifugal casting, thermal spraying, powder metallurgy, in-situ synthesis, adhesive bonding and self-propagating high temperature synthesis [14-16]. Among these techniques, centrifugal casting process was proven as an excellent processing method for FGM synthesis with limited casting defects [17,18]. The quality of centrifugal cast was dependant on many parameters such as amount of reinforcement particles, particle shape, particle size and solidification time [19]. An investigation on mechanical characteristics of functionally graded copper/10 wt.% WC (tungsten carbide) composite produced by centrifugal casting revealed improvement in hardness when compared to pure copper [20]. Efforts were made to study the wear behaviour of lead-free copper (90300)/13 vol.% graphite (5 μm) composite fabricated by centrifugal casting technique. Their results cemented that the fabricated composite had minimal material removal rate than base alloy under all applied loads [21]. Comparative analysis between 15 wt.% NbC (niobium carbide) reinforced copper composite synthesized through powder metallurgy showed that the hardness and wear resistance of composite was five times better compared to pure copper [22].

From above research, it is evident that mechanical and dry sliding wear study performed on functionally graded copper composite is limited. Hence, an extensive research is carried out to fabricate centrifuge cast, functionally graded copper composite reinforced 10 wt.% titanium carbide (TiC) and to investigate its mechanical and tribo-sliding characteristics.

2. EXPERIMENTAL PROCEDURES

The experimental procedures for composite fabrication, hardness, tensile and wear tests are detailed below:

2.1 Materials and Synthesis of composite

The materials used for the synthesis of functionally graded composite are Cu-Sn-Ni alloy and TiC particles as reinforcements. Copper was preferred as the matrix metal owing to its excellent strength (both tensile and yield), good hardness, good toughness, high corrosion resistance, along with excellent heat transfer coefficients. Density of copper is 8.94 g/cm^3 and its application includes use in condenser tubes, steam generator pipe in nuclear reactor, bearings, bushings and seashore environments. Addition of alloying elements such as Ni (density of 8.9 g/cm^3) and Sn (density of 7.27 g/cm^3) by 5 wt.% and 10 wt.% respectively, imparts improvement in mechanical properties, along with increase in corrosion and wear resistance. Ni has wide variety of applications, as in turbine vanes, fast breed reactors and jet engine components, whereas application of Sn involves in bearings, coatings and bells. 10 wt % TiC (30-40 μm) reinforcement particles were added into copper alloy in order to obtain properties like excellent thermal stability, thermal shock resistance, good inertness, good hardness, high tensile strength and high wear resistance. TiC is used in cutting tools, bearings, and wear resistant coatings.

Centrifugal casting was used to develop this composite. Initially, small copper rod was loaded onto a crucible and placed in a melting furnace

(Fig. 1) (with power capacity of 1200 W, 440 V, 3 phase) heated to a temperature of 1100 °C.

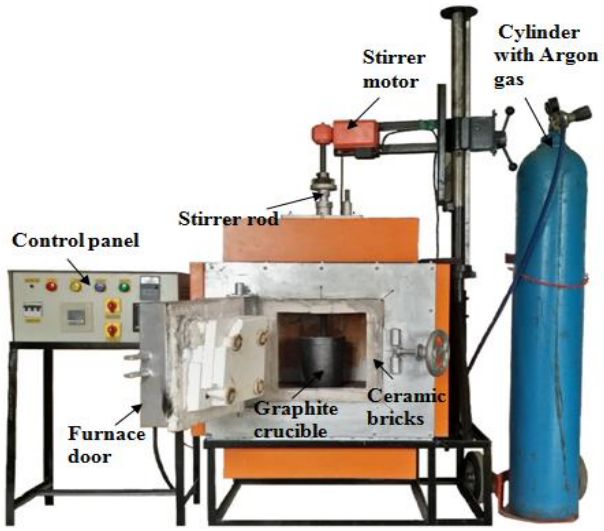

Fig. 1. Copper melting furnace.

a) Cylindrical section b) Longitudinal cross-section

Fig. 2. Cast composite sample.

Heating coil (12 mm diameter) made up of SiC was used for melting copper alloy. After melting of copper, small Sn ingots were added to the melt and made to dissolve. Followed by 5 wt.% of Ni was slowly dissolved in Cu-Sn melt at a temperature of 1200 °C in order to obtain a molten alloy under inert argon gas atmosphere. Through the hopper, preheated (250 °C) TiC particles were added into the molten metal and stirred using stirrer at 150 rpm. Then, the crucible containing molten metal was unloaded from the furnace and poured to a horizontal centrifugal mould preheated at 450 °C. This mould was rotating at 1000 rpm. After pouring, the melt transformed from liquid phase to solid phase due to decrease in temperature caused by cooling rate of the mould wall. Finally, hollow cylindrical cast was obtained with a dimension of Øout100 X Øin70 X 100 mm (Fig. 2) and was removed from die using an ejector.

2.2 Microstructure examination, hardness and tensile tests

Microstructure of composite specimens at outer (1 mm), middle (7 mm) and inner (15 mm) along radial wall thickness were studied using metallurgical (Zeiss Axiovert 25 inverted) microscope. Flat specimens of dimension 20 x 15 x 10 mm were initially rough polished using linisher polisher. Later using various emery paper grits (1/0, 2/0, 3/0), fine polishing was carried out on the flattened specimen to obtain a scratch free test domain. Then, final polish was performed to obtain a mirror finish surface of the specimen using an alumina solution impregnated velvet cloth fixed on top of a rotating grinder followed by etching with chemical reagents (2g $FeCl_3$ + 5ml HCl + 30ml water + 60 ml methanol). ImageJ software was used to analyse and compute the volumetric concentration of reinforcement particles along radial direction.

Micro-hardness measurements were carried out based on ASTM E 92 standards, along the radial direction of the functionally graded composite wall using Vickers micro hardness tester (Manufacturer: Mitutoyo & Series: HV-110A-810). Initially, specimen was polished with emery papers having grit size of 1/0, 2/0and 3/0 to remove scratches and to enhance the visibility of indentation on the surface of the specimen during testing. This test was performed with 500 g of applied load for 15s. Specimen was fixed on the anvil and load was applied by square based diamond pyramid, against the composite surface. The indentation on the specimen surface was measured after applying load for 15 s, to obtain the micro-hardness values. This was iterated for five times at different surface test spots and their average values were taken for final analysis.

Tensile strength was evaluated at both functionally graded composite inner and outer wall zones using Universal Testing (Tinius) Machine. ASTM E8 standards were used to prepare the tensile test specimens. Using the crossheads provided on the machine, the specimen was gripped tightly and load was gradually applied until fracture. During application of load, specimen was subjected to plastic deformation and fracture occurred by neck formation. This test was experimented under ambient temperature.

2.3 Tribology test

Adhesive tribo-experiments were conducted at three regions of the composite, namely outer, middle and inner, using pin-on-disc tribo-tester. Load, slide distance and slide velocity were the analytical parameters chosen for this experiment. The experiments were conducted by varying one parameter and by keeping the other two parameters constant. Initially, specimen was mounted on the specimen holder and was made to contact the hardened steel disc, where sliding occurred between two contact surfaces. Stainless steel EN32 is the disc material of 60-HRC, with an elemental composition of C (0.18 %), Mn (1 %), Si (0.35 %), P (0.05 %), S (0.05 %); and 8 mm thickness. Surface roughness (*R*a) of steel disc is determined as 1.6 µm. Five specimens were prepared for each cycle and their average result was used as reference for comparison cycle. Specimens were tested under varying loads of 10-40 N with 10 N step size, slide distance of 500-2000 m with 500 m step size and slide velocity of 1-4 m/s with 1 m/s variation. Burr free specimens were weighed (electronic balance) with a least count (LC) of 0.0001 g, before and after the experiment. Rate of wear was calculated from the weight loss that resulted after each cycle. To ensure fresh contact on the hardened steel disc, emery paper (1/0 and 2/0) polishing was done to remove the debris formed during previous cycles and this was done before each experiment cycle. Unchanged track diameter used for this test was 80 mm.

3. RESULTS AND DISCUSSION

Composite microstructure analysis, micro-hardness, tensile strength, dry slide tribo-characteristics and tribo-mechanisms observed are discussed in the subsequent sections.

3.1 Examination of Microstructure

Microstructure at inner, middle and outer wall regions is shown in Fig. 3. Microstructure of this composite reveals features like interfaces, grains, grain boundaries, triple junctions, and second phase particles (reinforcements). The dark phase depicts the grain boundary, whereas the white phase represents matrix. The dark coloured spherical shape particle represents the reinforcement particles. Microstructure at outer wall thickness (1mm) has least concentration (12 vol.%) of reinforcement particles (Fig. 3a).

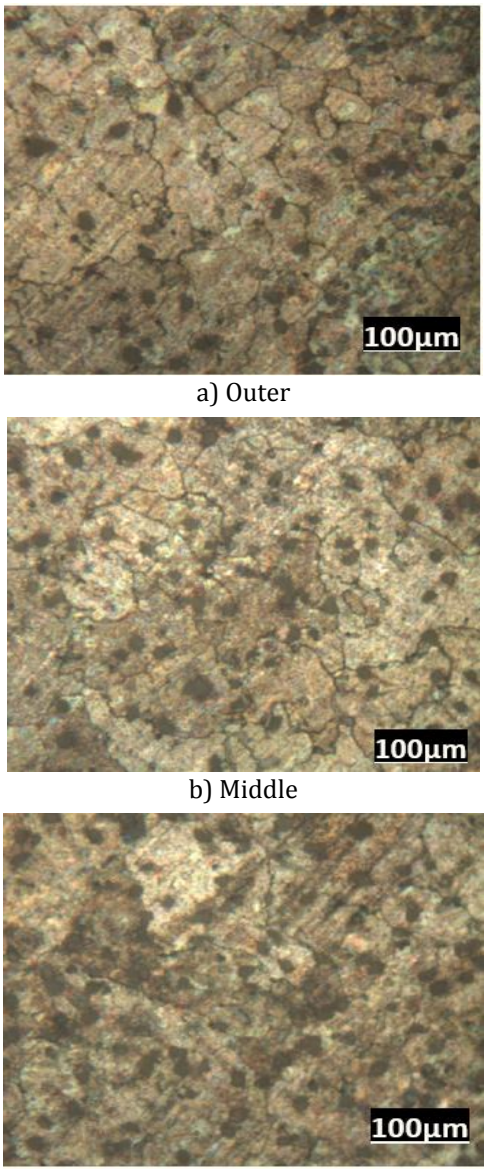

a) Outer

b) Middle

c) Inner

Fig. 3. Microstructure of copper FGM at different wall regions.

At middle region (7 mm), the reinforcement particle concentration (22 vol.%) was considerably higher as compared to outer region (Fig. 3b). This was due to the variance in density between the reinforcement particle and the matrix. Also, the rotating mould generates centrifugal force which would cause movement of particles towards inner region (15 mm). Also, the low density gases produced during casting assisted in the gradation of reinforcement particles, more towards inner region; resulting in higher concentration (39 vol.%) of reinforcement particles (Fig. 3c). This also

confirms supreme adhesion between matrix and reinforcement particles. In-spite of the density difference, the particle distribution undergoes gradation rather than accumulation at two extreme zones. This highlights the adhesiveness and bonding between the particle and matrix.

3.2 Evaluation of hardness

Hardness tests were conducted over the composite specimens at different radial wall distances from outer periphery and their results are depicted in Fig. 4.

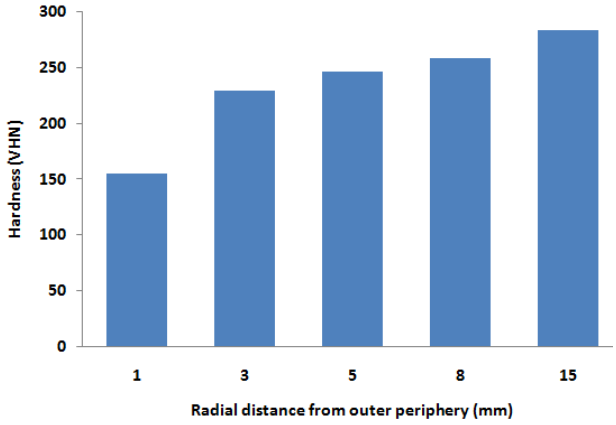

Fig. 4. Hardness of Cu- FGM along radial distance from outer periphery.

When the molten mixture is in direct contact with mould wall, the nucleation rate was found to be lower due to lower cooling rate due to conduction. This yields a coarser grain size and resulting in low hardness (155 HV) at 1 mm radial wall thickness from exterior surface. As the radial distance increased from 1 to 3 mm, the hardness of composite also increased. This is owing to the higher cooling rate due to conductive and convective heat transfer occurring along the wall and atmospheric interface respectively. This resulted in finer grains, providing a large hindrance for granular dislocation under loaded condition, thereby increasing hardness. Furthermore, owing to the thermal contraction occurring between matrix and TiC particles, an increase in hardness of composite was obtained when distance increased from 3 to 8 mm, resulting in quench hardening effect. During solidification, the grain propagation is obstructed by the presence of TiC particles unevenly distributed in the melt, which acted as sites for heterogeneous nucleation. Hence, fine grains are formed at the inner regions (i.e. 15 mm radially from the outer periphery) which ended up with higher value of hardness (284 HV). When load was applied, the dislocation movement took place and dislocation bent was formed around the particle to form a loop, by Orowan looping mechanism. As a result, an improvement in hardness was observed owing to the strain created by the formed loop over the adjacent lattice.

3.3 Evaluation of tensile strength

Two composite zones were considered for performing tensile test i.e. inner and outer. Sample from inner wall exhibited higher ductile strength (291 MPa) than the outer (236 MPa). This was due to the lesser volume percentage of reinforcement particles at the outer zone, which reduces the tensile strength of the composite causing smooth granular dislocation movement. Inner region had higher volume distribution of particles, which provided a huge hindrance for nucleation and growth of voids. Also, necking was delayed at inner zone, due to gradation of higher volume fraction of reinforcement particles and thus enhancing tensile strength.

3.4 Fractography

SEM analysis on broken sections of tensile test for both inner and outer wall zones of the composite reveals (Fig. 5) the fracture mechanism occurred during tensile test. In outer zone of composite, ductile mode of fracture was observed. This was interpreted by the appearance of fibrous and dimples (Fig. 5a). Fracture occurred as this zone had minimal presence of reinforcement particles which hindered the plastic deformation. The mechanism for ductile fracture involves three stages; they are nucleation, growth and propagation of voids. When the load was applied on the composite, void formations were observed at locations where there existed heterogeneous sites (inclusion, porosity and blow holes, etc.). At inner zone of the composite (Fig. 5b), combined action of brittle and ductile mode caused failure. The presence of cracks and facets observed is counted as an evidence for brittle mode failure. Cracks were nucleated by presence of heterogeneities such as depressions, striation, holes, and steps which acted as stress concentration sites. These cracks propagated along their specified crystallographic direction due to release of strain energy, which act as driving force for propagation.

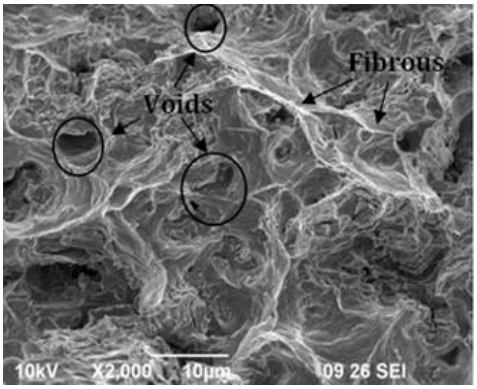

a) Outer zone

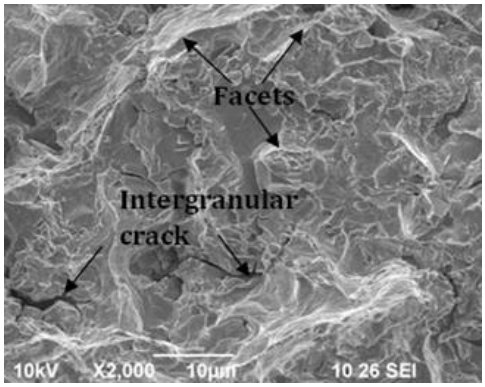

b) Inner zone

Fig. 5. Fractography analysis on broken section of tensile test.

The inter-crystalline cracks formed due to voids were located preferentially along their grain boundaries. Brittle failure was also predicted when interatomic bonds were broken at maximum loading, resulting in pull out of reinforcements, crack nucleation, propagation and final rupture.

3.5 Relation of load with composite wear rate

Variation in rate of wear at all three zones of the composite wall is illustrated in Fig. 6, keeping sliding distance and sliding velocity unchanged at 1000 m and 2 m/s respectively. The increase in composite wear at the inner region with respect to load was minimal compared with other regions of the composite. At outer region, due to less particle presence, the counter body was in direct contact with matrix, which produced high heat and thus increased the wear. At middle region, partial contact between matrix and counter body was observed, as majority of the contact of counter body was made with hard reinforcement particles. Thus, the middle region of copper FGM exhibited lesser wear as compared to outer region. Out of all these composite wall regions, inner region exhibited minimum wear. This is because, at low load (10 N) the heat generation was also low, due to minimal contact between composite and rotating disk. Also, the strain developed at the sub surface layer due to the applied load was significantly less which resulted in minimum wear. As the load increased (10 N to 20 N), the contact of counter body with composite also increased which resulted in rise of wear. With further increase in load (20 to 30 N), composite wear increased furthermore due to larger friction between the mating surfaces. Composite subsurface underwent plastic deformation at superior load (40 N) due to the deterioration or rupture of reinforcement particles at extreme loading. At higher loads, it is often observed that particles are broken or pull-out from matrix, when in combination with slide velocity (2 m/s). This has induced slight plasticity at the matrix level which in turn promoted particle release. This resulted in higher wear rate, observed at extreme load (40 N) conditions.

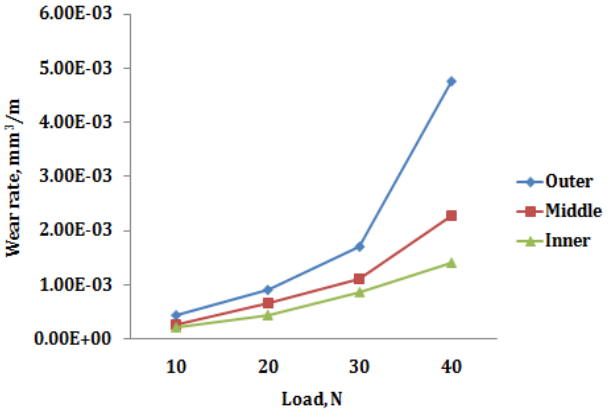

Fig. 6. Relation of Load with rate of wear.

On experimental investigation, it was observed that the anti-tribo performance of composite was superior at inner wall zone and this led to the analysis of wear mechanism at this zone. SEM analysis revealed the effect of applied load on worn surfaces of composite. The presence of small patch of tribolayer formation (Fig. 7a), was considered responsible for the occurrence of mild wear at least load condition (10 N). This tribo-mechanism was exhibited due to the combined effect of slight oxidation of copper composite during sliding along with the limited transfer of counter body material on specimen surface. Kubota [23] reported a similar inference in an earlier study.

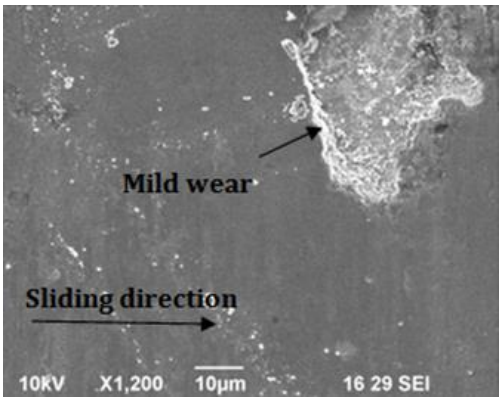

a) 10 N

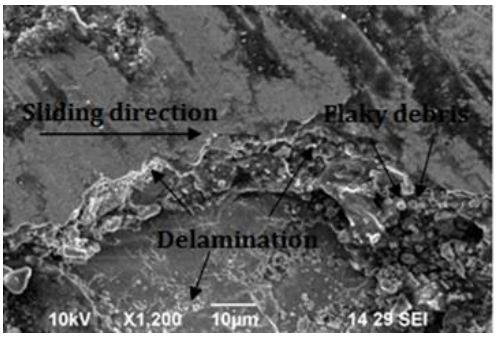

b) 40 N

Fig. 7. Worn composite specimen at varied loads.

At a superior load (40 N) (Fig. 7b), the composite experienced high wear on specimen surface. This occurred as a result of delamination and ploughing phenomenon, as observed. Repeated sliding action in the presence of wear debris and counter body resulted in delamination. During sliding, two classes of wear debris were formed in composite such as coarse flaky and fine equiaxed debris**.** Large sized flaky wear debris (Fig. 7b) formation was observed at high load, which was a clear indication of delamination wear. A similar observation was also quoted by Mandal [24] with A356–TiB_2 in-situ composites. Work hardening on the composite surface, caused by severe plastic deformation due to high pressure contact was also attributed to increased wear rate of composite.

3.6 Relation of sliding distance with composite wear rate

Outer wall zone of the composite experienced higher rate of wear (Fig. 8) at each slide distance, followed by middle and inner regions. The inner wall zone revealed least wear rate at the lowest slide distance (500 m), keeping load (20 N) and slide velocity (2 m/s) unchanged. This was due to the higher presence of wear resistant reinforcements present at this zone. Whereas, the outer region of composite had least volume fraction of reinforcement particles, limiting the action of resisting force against wear. This resulted in enhanced rate of wear on the outer wall zone of the composite. Middle zone showed proportional rise in wear rate with respect to the increase in slide distance, at different rates. At minimum range of slide distance (500-1000 m), the rigidity of reinforcement particles restricted direct contact of matrix with counter body. This also led to withstanding of contact stresses, resulting in minimum wear for all three wall zones. Among which, inner and outer zones showed least and highest rate of wear. Shoot up of wear rates were observed for both outer and middle wall zones; at different rates along slide ranges of 1000-1500 m and 1500-2000 m respectively. This was owing to the cracking phenomenon observed with the low volume fraction of reinforcement particles at these zones compared to inner. As slide distance increased from 500 to 2000 m, inner zone revealed multiple cross links in trend-line, with that of middle zone. This is because, the rate of wear exhibited at these slide conditions were same for both inner and middle wall zone. A considerable rise in wear is observed at middle wall zone, as particles pull out from matrix to cause direct matrix contact, while increasing the slide distance (1500 to 2000 m).

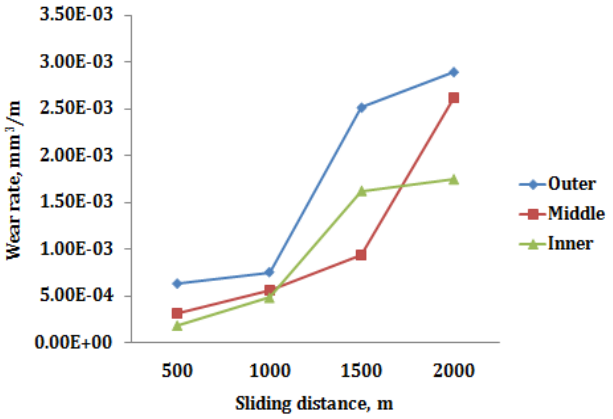

Fig. 8. Relation of sliding distance with rate of wear.

SEM morphology (Fig. 9) of pin surface prepared from inner composite wall layers, were analysed for different sliding distances. This revealed that at low sliding distance (500 m), the presence of reinforcement particles caused shallow wear track (Fig. 9a).

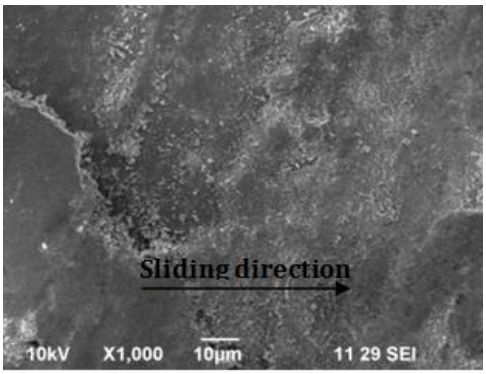

a) 500 m

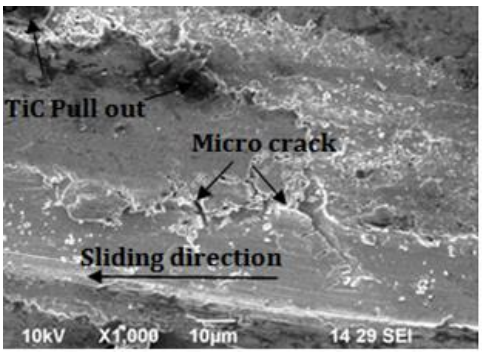

b) 2000 m

Fig. 9. Worn composite specimen at varied sliding distances.

This was because these particles prevented direct contact of counter face with the matrix. By increasing sliding distance up to 2000m, the hard reinforcement particles could not sustain a huge amount of shear stress, which resulted in nucleation of micro crack on the reinforcements. Such micro crack grows along their sliding direction caused dislodging of the reinforcement particles (Figure 9b) from copper matrix. This led the sliding contact to move towards the matrix and thereby, resulted in increased material removal. Hence, it is concluded that micro cutting and ploughing were the main wear mechanisms for high sliding distance and a similar result is reported by Jahangiri [25], while investigating the influence of energy dissipation on sliding tribo-performance of materials.

3.7 Relation of sliding velocity with composite wear rate

Relation of slide velocity on tribology is shown in Fig. 10, at all three wall zones of the composite, keeping slide distance (1000 m) and load (20 N) unchanged. It is inferred that, as slide velocity increases, an increase in wear was seen at outer and middle regions of the composite, while a decrease in wear rate was reflected at the inner region. For outer and middle regions of composite, a proportional rise in wear was observed with sliding velocity at different rates. This is because of the less concentration of reinforcement particles along the radial wall which prevents the direct contact of the counter surface of the matrix [26]. Whereas in case of inner region, even at low slide velocity (1 m/s) and high particle presence, the rate of wear was observed as high. This was because of the third body abrasive wear induced by the broken reinforcement particles at the slide interface during high velocity. During repeated cycles, the fracture of reinforcement particles released a thin stable lubricating surface film over the composite surface. Thus, the wear rate correspondingly decreased steeply as velocity increased from 1 to 3 m/s. Beyond which a further gradual decrease in rate of wear occurred at inner wall zone as a result of inhabitancy of direct interfacial slide contact between matrix and counter body [27].

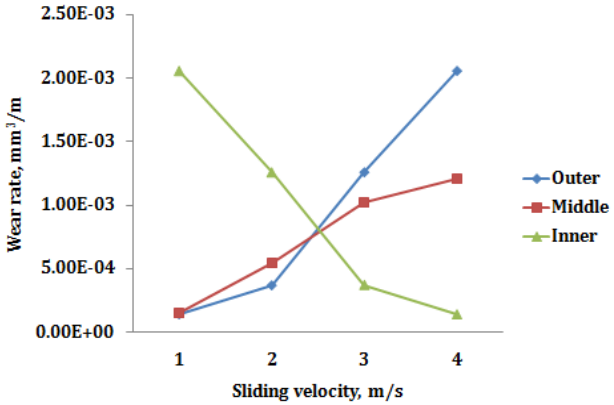

Fig. 10. Relation of sliding velocity with rate of wear.

Figure 11 shows SEM analysis on worn specimen from inner wall zone. At 1 m/s sliding velocity, the inner composite wall zone was prone to higher rate of material removal, this was characterized by the presence of deep grooves, tracks of wear marks and fatigue layers. The high wear rate at this velocity was also attributed to the generation of large shear stress on the composite subsurface layer. By increasing the sliding velocity to 4 m/s, a considerable decline in material removal rate was observed since the formation of thin film of lubrication which prevented the contact between mating surfaces. This thin formation occurred when the reinforcement particles were crushed and resulted in formation of wear debris.

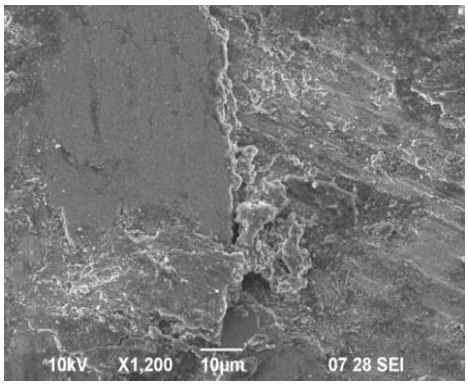

a) 1 m/s

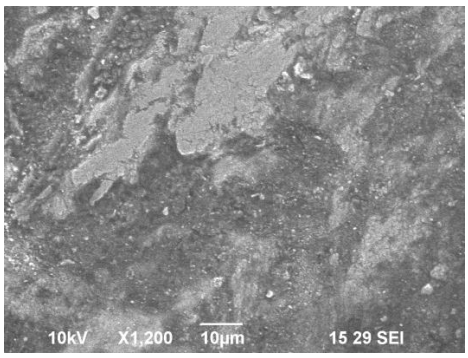

b) 4 m/s

Fig. 11. Worn composite specimen at varied sliding velocities.

These debris were further rolled between mating surfaces and consequently a stable lubricating film was formed. This thin film adhered with the matrix interface was not collapsed even at higher sliding velocity.

4. CONCLUSION

TiC reinforced functionally graded copper composite was successfully synthesized via centrifugal casting route. The mechanical and tribological experiments conducted on the fabricated composite, revealed the below:

1) Based on microstructure examination, inner region of the composite had more volume fraction of reinforcement particles as a result of centrifugal action due to die rotation and also due to matrix-reinforcement particle density difference.
2) The reinforcement particle concentration varies from outer to inner periphery. Vickers micro hardness analysis indicated that hardness increased proportionally along the radial wall of composite towards inner periphery.
3) Results of tensile strength showed that inner zone had higher tensile strength due to effective gradient structure on the composite as compared to the outer zone. Also, restriction to the dislocation movement was high at inner region of composite which also attributed to raise the tensile strength. Outer zone fractography analysis revealed ductile mode of failure, while at inner zone the sample fracture involved a combination of both brittle and ductile failure.
4) Based on wear experimental results, with addition of applied load and slide distance, wear increased. Inner region of composite displayed minimal amount of material removal. The wear rate at both outer and middle regions increases as sliding velocity increases. However, wear rate decreased for inner region, owing to the formation of thin lubricating layer.
5) Using scanning electron microscopy, worn surfaces were analysed and it revealed that ploughing, particle pull-out, plastic deformation with flaky wear debris and thin film formation were the significant wear mechanisms involved during wear experiments.

Acknowledgement

We owe our sincere thankfulness to Defence Research and Development Organization (DRDO) for providing the funding support at each stage of this research.

REFERENCES

[1] C. Suryanarayana, *Mechanical behavior of emerging materials*, Materials Today, vol. 15, iss. 11, pp. 486-498, 2012, doi: 10.1016/S1369-7021(12)70218-3

[2] N. Radhika, R. Subramanian, *Effect of reinforcement on wear behaviour of aluminium hybrid composites*, Tribology-Materials, Surfaces & Interfaces, vol. 7, iss. 1, pp. 36-41, 2013, doi: 10.1179/1751584X13Y.0000000025

[3] J.H. You, *Copper matrix composites as heat sink materials for water-cooled divertor target,* Nuclear Materials and Energy, vol. 5, pp. 7-18, 2015, doi: 10.1016/j.nme.2015.10.001

[4] V. Rajkovic, D. Bozic, M.T. Jovanovic, *Properties of copper matrix reinforced with nano-and micro-sized Al_2O_3 particles*, Journal of Alloys and Compounds, vol. 459, iss. 1-2, pp. 177-184, 2008, doi: 10.1016/j.jallcom.2007.04.307

[5] T. Schubert, A. Brendel, K. Schmid, T. Koeck, W. Zieliński, T. Weißgärber, B. Kieback, *Interfacial design of Cu/SiC composites prepared by powder metallurgy for heat sink applications*, Composites Part A: Applied Science and Manufacturing, vol. 38, iss. 12, pp. 2398-2403, 2007, doi: 10.1016/j.compositesa.2007.08.012

[6] K. Deenadayalan, V. Murali, *Role of various weight percentages of WC particle on interface thickness and friction-wear property of NiCrBSi-WC composite fabricated using PTAW process*, Material Research Express, vol. 6, 2019, doi: 10.1088/2053-1591/aafd4f

[7] M. Naebe, K. Shirvanimoghaddam, *Functionally graded materials: A review of fabrication and properties*, Applied Materials Today, vol. 5, pp. 223-245, 2016, doi: 10.1016/j.apmt.2016.10.001

[8] R. Murakami, K. Matsui, *Evaluation of mechanical and wear properties of potassium acid titanate whisker-reinforced copper matrix composites formed by hot isostatic pressing*, Wear, vol. 201, iss. 1-2, pp. 193-198, 1996, doi: 10.1016/S0043-1648(96)07239-0

[9] L. Liu, Y. Tang, H. Zhao, J. Zhu, W. Hu, *Fabrication and properties of short carbon fibers reinforced copper matrix composites*, Journal of Materials Science, vol. 43, iss. 3, pp. 974-979, 2008, doi: 10.1007/s10853-007-2089-5

[10] Y. Zhan, G. Zhang, Y. Zhuang, *Wear transitions in particulate reinforced copper matrix composites*, Materials Transactions, vol. 45, no. 7, pp. 2332-2338, 2004, doi: 10.2320/matertrans.45.2332

[11] J.Y. Wu, Y.C. Zhou, J.Y. Wang, *Tribological behavior of Ti_2SnC particulate reinforced copper matrix composites*, Materials Science and Engineering: A, vol. 422, iss. 1-2, pp. 266-271, 2006, doi: 10.1016/j.msea.2006.02.010

[12] R. Cui, Y. Han, Z. Zhu, B. Cheng, Y. Ding, Q. Zhang, Q. Wang, G. Ma, F. Pei, Z. Ye, *Investigation of the structure and properties of electrodeposited Cu/graphene composite coatings for the electrical contact materials of an ultrahigh voltage circuit breaker*, Journal of Alloys and Compounds, vol. 777, pp. 1159-1167, 2019, doi: 10.1016/j.jallcom.2018.11.096

[13] N. Radhika, R. Raghu, *Mechanical and tribological properties of functionally graded aluminium/zirconia metal matrix composite synthesized by centrifugal casting*, International Journal of Materials Research, vol. 106, iss. 11, pp. 1174-1181, 2015, doi: 10.3139/146.111293

[14] L. Prchlik, S. Sampath, J. Gutleber, G. Bancke, A.W. Ruff, *Friction and wear properties of WC-Co and Mo-Mo_2C based functionally graded materials*, Wear, vol. 249, iss. 12, pp. 1103-1115, 2001, doi: 10.1016/S0043-1648(01)00839-0

[15] B. Kieback, A. Neubrand, H. Riedel, *Processing techniques for functionally graded materials*, Materials Science and Engineering: A, vol. 362, iss. 1-2, pp. 81-106, 2003, doi: 10.1016/S0921-5093(03)00578-1

[16] J. Singh, A. Chauhan, *A review of microstructure, mechanical properties and wear behavior of hybrid aluminium matrix composites fabricated via stir casting route*, Sadhana, vol . 44, p. 16, 2019, doi: 10.1007/s12046-018-1025-5

[17] D. Xue, Y. Jia, X. Zhang, Y. Jiang, Y. Sui, *Effect of ZTA volume fractions on the microstructure and properties of ZTAp/high manganese steel composites,* Material Research Express, vol. 6, no. 4, 2019, doi: 10.1088/2053-1591/aafbf2

[18] J.J. Sobczak, L. Drenchev, *Metallic functionally graded materials: A specific class of advanced composites*, Journal of Materials Science & Technology, vol. 29, iss. 4, pp. 297-316, 2013, doi: 10.1016/j.jmst.2013.02.006

[19] N. Radhika, R. Raghu, *Development of functionally graded aluminium composites using centrifugal casting and influence of reinforcements on mechanical and wear properties*, Transactions of Nonferrous Metals Society of China, vol. 26, iss. 4, pp. 905-916, 2016, doi: 10.1016/S1003-6326(16)64185-7

[20] M. Kestursatya, J.K. Kim, P.K. Rohatgi, *Friction and wear behavior of a centrifugally cast lead-free copper alloy containing graphite particles*, Metallurgical and Materials Transactions A, vol. 32, iss. 8, pp. 2115-2125, 2001, doi: 10.1007/s11661-001-0023-z

[21] S.G. Shiri, P. Abachi, K. Pourazarang, M.M. Rahvard, *Preparation of in-situ Cu/NbC nanocomposite and its functionally graded behavior for electrical contact applications*, Transactions of Nonferrous Metals Society of China, vol. 25, iss. 3, pp. 863-872, 2015, doi: 10.1016/S1003-6326(15)63675-5

[22] N.B. Dhokey, R.K. Paretkar, *Study of wear mechanisms in copper-based SiC_p (20% by volume) reinforced composite*, Wear, vol. 265, iss. 1-2, pp. 117-133, 2008, doi: 10.1016/j.wear.2007.09.001

[23] Y. Kubota, S. Nagasaka, T. Miyauchi, C. Yamashita, H. Kakishima, *Sliding wear behavior of copper alloy impregnated C/C composites under an electrical*

current, Wear, vol. 302, iss. 1-2, pp. 1492-1498, 2013, doi: 10.1016/j.wear.2012.11.029

[24] A. Mandal, B.S. Murty, M. Chakraborty, *Sliding wear behaviour of T6 treated A356–TiB_2 in-situ composites*, Wear, vol. 266, iss. 7-8, pp. 865-872, 2009, doi: 10.1016/j.wear.2008.12.011

[25] M. Jahangiri, M. Hashempour, H. Razavizadeh, H.R. Rezaie, *A new method to investigate the sliding wear behaviour of materials based on energy dissipation: W–25wt% Cu composite*, Wear, vol. 274-275, pp. 175-182, 2012, doi: 10.1016/j.wear.2011.08.023

[26] M. Sam, N. Radhika N, *Effect of Heat Treatment on Mechanical and Tribological Properties of Centrifugally Cast Functionally Graded Cu/Al_2O_3 Composite*, Journal of Tribology, vol. 140, iss. 2, p. 7, 2017, doi: 10.1115/1.4037767

[27] Y. Fang, Y. Zhang, J. Song, H. Fan, L. Hu, *Influence of structural parameters on the tribological properties of Al_2O_3/Mo laminated nanocomposites*, Wear, vol. 320, pp. 152-160, 2014, doi: 10.1016/j.wear.2014.09.003